Dyes and Pigments 101 (2014) 254–260

Contents lists available at ScienceDirect

Dyes and Pigments

journal homepage: www.elsevier.com/locate/dyepig

Rhodamine based colorimetric and fluorescent probe for recognition of nucleoside polyphosphates through multi-hydrogen bond

Jichuan Kong [a,b,1], Cheng He [a,1], Xiaolin Zhang [a,1], Qingtao Meng [a,1], Chunying Duan [a,*]

[a] State Key Laboratory of Fine Chemicals, Dalian University of Technology, 158 Zhongshan Road, Dalian 116012, China
[b] Institute of Physics and Chemistry, Henan Polytechnic University, Jiaozuo 454000, China

ARTICLE INFO

Article history:
Received 28 August 2013
Received in revised form
28 September 2013
Accepted 2 October 2013
Available online 18 October 2013

Keywords:
Chemosensor
Nucleoside
Colorimetric and fluorescent
Naphthyridine
Rhodamine B
Cell imaging

ABSTRACT

A novelty rhodamine B based chemosensor containing 2-amino-7-methyl-1, 8-naphthyridine moiety was designed and synthesized for colorimetric and fluorescent response on corresponding nucleoside polyphosphates through multi-hydrogen bond interaction in aqueous solution. The supramolecular recognition between the **RBS** and Cytidine-5′-diphosphate disodium hydrate (CDP) was investigated carefully: ^{1}H nuclear magnetic resonance confirmed that the formation of multi-hydrogen bonds between naphthyridine moiety and the nucleoside base group could untie the spiro structure of **RBS**, and the ESI-MS spectra proved the formation of the 1:1 complexation species between **RBS** and CDP. The strong emission response of the **RBS** toward CDP and Adenosine-5′-triphosphate disodium trihydrate (ATP) ensures its application in living cells imaging.

1. Introduction

The design of artificial molecular receptor for the recognition of nucleotide polyphosphates is very important since nucleotide polyphosphates play pivotal roles in various physiological events, such as transport across membranes, **DNA** synthesis, cell signaling and energy processes [1,2]. As the well known paragon, hydrogen bonds between purine and pyrimidine bases which contribute to delicate double helical structure of **DNA**, played important role in the supramolecular recognition of nucleotide polyphosphates. To realize the recognition for the nucleotides, constructing effectively hydrogen bonding platform to act as artificial receptor molecules could be judicious strategy. The 2-amino-1,8-naphthyridine derivatives shown to bind effectively with guanine or cytosine *via* triple hydrogen bonding mode [3–6] in accordance with the different microenvironment, respectively, have been well used in construction of efficient molecular sensors for nucleotide polymorphism.

On the other hand, the detection of nucleotide polyphosphates in real time and *in vivo* has gained particular importance to understand their physiological roles and the application in medicine. [7] Fluorescence measurement of specific biological molecules by artificial chemosensors, as a versatile technique with high sensitivity, rapid response, and easy performance, offering utility not only for in vitro assays but also for *in vivo* imaging studies, is a promising technique for elucidation of biological functions of nucleotide polyphosphates [8]. However, 1,8-naphthyridine itself with low quantum yields (0.01 *vs* **Rh6G**) is difficult to monitor biological events sensitively.

Because of the large molar extinction coefficient and the high fluorescence quantum yield, rhodamine-based dyes have been used as effective dual responsive optical probes *via* chromogenical and fluorogenical signals [9–13]. Herein, by incorporating 2-amino-7-methyl-1,8-naphthyridine (**AMND**) into the rhodamine B group, the colorless and nonfluorescent spirolactam platform could be obtained. Additionally, **AMND** possessing hydrogen bonding sites could form multiple hydrogen bonds with nucleic acid base. Herein, we use rhodamine B spirolactam complex with **AMND** as a new and practical luminescence chemosensor (**RBS**) for the detection of nucleoside polyphosphates in aqueous solution and in living systems with high contrast to background. Since rhodamine B is a promising signaling subunit emitting in the red region with high quantum yields, the chemosensor is also successfully applied to cells imaging for related nucleotide polyphosphates, respectively.

* Corresponding author. Tel./fax: +86 411 84986216.
E-mail address: cyduan@dlut.edu.cn (C. Duan).
[1] Tel./fax: +86 411 84986216.

0143-7208/$ – see front matter © 2013 Elsevier Ltd. All rights reserved.
http://dx.doi.org/10.1016/j.dyepig.2013.10.002

2. Experiment

2.1. Materials and methods

All the reagents and solvents unless otherwise stated, were purchased from commercial sources and used without further purification. Adenosine-5′-triphosphate disodium trihydrate (**ATP**), Adenosine-5′-diphosphate disodium (**ADP**), Adenosine-5′-monophosphate acid monodydrate (**AMP**), Cytidine-5′-triphosphate disodium dihydrate (**CTP**), Cytidine-5′-diphosphate disodium hydrate (**CDP**), Cytidine-5′-diphosphate acid (**CMP**), Guanosine-5′-triphosphate disodium hydrate (**GTP**), Guanosine-5′-diphosphate disodium (**GDP**), Guanosine-5′-monophosphate disodium (**GMP**), Uridine-5′-triphosphate trisodium (**UTP**), Uridine-5′-diphosphate disodium (**UDP**) and Uridine-5′-monophosphate disodium (**UMP**) were purchased from Bio Basic Inc. (**BBI**) company. ^{1}H NMR spectra were measured on a VARIAN INOVA-400 spectrometer with chemical shifts reported as ppm (in d_6-DMSO, $CDCl_3$ or D_2O, TMS as internal standard). ESI mass spectra were carried out on an HPLC-Q-Tof MS spectrometer. The solution fluorescent spectra were measured on EDINBURGH FS920. Optical absorption spectra were measured on a TU-1900 Uv−Vis spectrophotometer at room temperature. The fluorescence imaging for intracellular nucleoside polyphosphates in HeLa cells was observed under Nikon eclipse TE2000-5 inverted fluorescence microscopy with a 20× objective lens (excited with green light) and Olympus FV1000 laser scanning microscopy with a 40× objective lens (excited with 510 nm).

Single crystals data of compound **RBS** was collected on a BRUKER SMART APEXCCD diffractometer with graphite-monochromated Mo-Kα (λ = 0.71073 Å) using the SMART and SAINT programs. The skeleton non-hydrogen atoms were refined anisotropically and hydrogen atoms within the ligand backbones were fixed geometrically at calculated distances and allowed to ride on the parent non-hydrogen atoms.

Cell imaging was measured on Nikon eclipse TE2000-5 inverted fluorescence microscopy and Olympus FV1000 laser scanning microscopy. HeLa cells were cultured in 1640 supplemented with 10% FCS (Invitrogen). Cells were seeded on 18 mm glass cover slips for fluorescence imaging and in 24-well flat-bottomed plates. After 12 h, HeLa cells were incubated with 10 μM compound **RBS** buffer solution (pH = 6.04) for 30 min at room temperature and then washed with physiological brine three times before incubating with 40 eq nucleoside polyphosphates (pH = 6.04) for another 30 min, and cells were rinsed with physiological brine three times again. The fluorescence imaging of intracellular nucleoside polyphosphates in HeLa cells was observed under Nikon eclipse TE2000-5 inverted fluorescence microscopy with a 20× objective lens (excited with green light) and Olympus FV1000 laser scanning microscopy with a 40× objective lens (excited with 510 nm).

The binding constant was calculated from the fluorescent titration curve according to the equation.

$$\mathrm{Log}((F - F_{\min})/(F_{\max} - F)) = \log k + n \log[c]$$

where F is fluorescent intensity of **RBS** at 583 nm upon the addition of different amount of nucleoside polyphosphates. [c] stands for the concentration of nucleoside polyphosphates.

2.2. Synthesis of 2-amino-7-methyl-1,8-naphthyridine (*AMND*) [14,15]

2,6-Diaminopyridine (3.00 g, 27.5 mmol) was dissolved in 35 mL of H_3PO_4 at 90 °C under Ar atmosphere, 3-ketobutanal dimethyl acetal (3.70 g, 28.2 mmol) was slowly added from a pressure-equalizing addition funnel, and the mixture was heated at 115 °C. Reactions were monitored by TLC. After cooling, neutralized with NH_4OH (15%) and sodium hydroxide until pH = 8, extracted with $CHCl_3$ for several times, while the extraction solution was monitored, washed with brine, dried over anhydrous magnesium sulfate, and concentrated to yield a dark-red solid which was recrystallized from toluene to afford 2.30 g of the products (52%); ^{1}H NMR ($CDCl_3$, ppm): 7.82 (d, 1H, J = 4.0 Hz), 7.80 (d, 1H, J = 4.0 Hz), 7.07 (d, 1H, J = 8.0 Hz), 6.71 (d, 1H, J = 8.4 Hz), 5.08 (s, 2H), 2.69 (s, 3H).

Table 1
Crystal data and structure refinement for **RBS**.

Empirical formula	C_{37} $H_{39.50}$ N_5 $O_{3.25}$
Formula weight	606.24
Crystal size	0.24 × 0.26 × 0.28 mm^3
Temperature (K)	293(2)
Wavelength (Å)	0.71073 Å
Crystal system	Monoclinic
Space group	*C*2/*c*
a(Å)	24.7312(12)
b(Å)	25.7108(12)
c(Å)	20.9872(12)
β(deg)	91.845(4)
V(Å^3)	13,338.0(12)
Z	16
Dc(g cm^{-3})	1.208
μ(mm^{-1})	0.078
F(000)	5160
Theta range for data collection	1.86–25.00 deg.
Reflections collected	34,605
Independent reflections	11,668 (Rint = 0.0470)
Completeness to theta = 25.00	99.2%
Absorption correction	None
Refinement method	Full-matrix least-squares on F^2
Goodness-of-fit on F^2	1.031
Final Rindices [$I > 2\sigma(I)$]	R_1 = 0.0845[a], wR_2 = 0.2178[a]
Rindices (all data)	R_1 = 0.2180[a], wR_2 = 0.2546[a]
Largest peak and hole (e Å^{-3})	0.453 and −0.277
CCDC number	954044

[a] $R_1 = \sum(|F_0| - |.F_c|.)/\sum|.F_0|.$; $wR_2 = [\sum w(|F_0| - |.F_c|.)^2/\sum wF_0^2]^{1/2}$.

2.3. Synthesis of *RBS* [16–18]

To a solution of rhodamine B (1.0 g, 2.1 mmol) in dry 1,2-dichloroethane (15 mL) under stirring phosphorus oxychloride (1.9 mL, 21 mmol) was added dropwise over a period of 10 min, with a pressure-equalizing addition funnel under Ar. After being heated to reflux for 4 h, the solvent and excess amount of phosphorus oxychloride was removed by rotary evaporation to give the corresponding acid chloride, which was dried over high vacuum and used for the next step without further purification. To a solution of the acid chloride in dry acetonitrile (5.0 mL) was added dropwise a solution of **AMND** (0.5 g, 3.15 mmol) and triethylamine (5 mL) in dry acetonitrile (10.0 mL), the resulting mixture was heated to reflux for 5 h. The reaction mixture was then concentrated under vacuum, and the residue was purified by column chromatography (ethyl acetate/dichloromethane 1/1, v/v) to give the crude product, which was further purified by recrystallization from dichloromethane/hexane (25/1, v/v) to give a pure compound **RBS** as a white solid in 22% yield (0.275 g); ^{1}H NMR (d_6-DMSO, ppm): 1.03 (12H, m), 2.57 (3H, s), 3.24–3.34 (8H, m), 6.15 (1H, d, J = 2.6 Hz), 6.17 (1H, d, 2.6, J = 8.8 Hz), 6.40 (4H, m), 7.05 (1H, d, J = 8.8 Hz), 7.32 (1H, d, J = 7.7 Hz), 7.59 (1H, t, 8.8 Hz), 7.64 (1H, t, J = 7.7 Hz), 7.97 (1H, d, J = 7.2 Hz), 8.12 (1H, d, J = 8.0 Hz), 8.25 (1H, d, J = 8.8 Hz), 8.47 (1H, d, J = 8.8 Hz); ^{13}C NMR 168.67, 162.27, 154.63, 154.20, 153.52, 152.57, 148.50, 137.32, 135.75, 133.73, 129.90, 128.12, 128.05, 124.30, 123.41, 121.35, 118.25, 116.04, 107.98, 107.40, 98.01, 66.85, 44.26, 25.60, 12.61; TOF-ESI-MS: Calcd for $[M + 2H]^{2+}$: 292.6552 *m/z*. Found: *m/z* 292.7144; Calcd for $[M + H]^+$: *m/z* 584.3026. Found: *m/z* 584.4264.

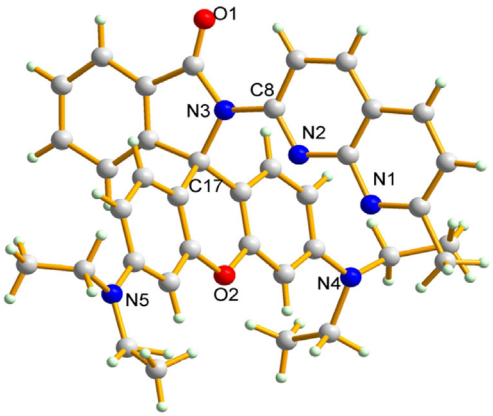

Fig. 1. Crystal structure of molecule **RBS**. Solvent molecules and disorder parts are omitted for clarity.

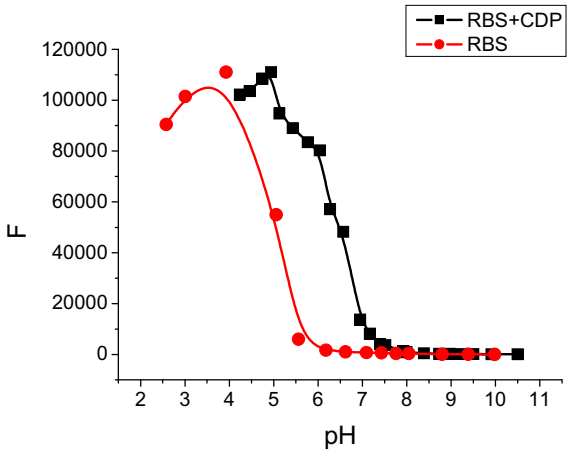

Fig. 2. Effects of pH on the fluorescence intensity of 1 (10 μM) in the absence and presence of **CDP** (10 eq).

3. Results and discussion

3.1. Characteristics of *RBS*

Compound **RBS** was obtained as a colorless and nonfluorescent product. ^{13}C NMR spectrum of **RBS** showed the characteristic spirolactam form with the chemical shifts of the signals at $\delta = 66.85$ ppm. Single crystals of **RBS** were got from evaporating a dichloromethane/acetonitrile solution. Crystal data and details on data collection and refinement are summarized in Table 1. X-ray structure analysis reveals that amino group on the **AMND** was incorporated into the rhodamine B spirolactam ring (Fig. 1), and the best common plane between spirolactam ring and **AMND** with deviation 0.027 Å is almost perpendicular to the xanthenes plane with the angle being 91.1°. The angle between C8-N3 and C17-N3 is 122.3°. Such steric configuration could facilitate the fluorescent recognition of **RBS** toward nucleotide bases. The spirocycle will be opened when the amide group contained **AMND** moiety form hydrogen bond pair with suitable guest (Scheme 1).

It is well known that rhodamine spiroamides on–off conversion strongly depends on the pH value in environment solution system [19–21]. Its spirolactam form could not be stable in a strong acid environment. At the meantime, the relative tiny interaction energy resulting from hydrogen bonds was no less than −21.0 kcal M^{-1} [22–25] and also significantly suppressed by hydration of the binding site [26]. As a result, rhodamine spiroamides could not open up in basic solution regardless of the complementary hydrogen bonding between **AMND** and nucleic acid base. Hence, the Tris–HCl buffer solution with pH being 6.04 was selected for the spectral investigation based on the acid–base

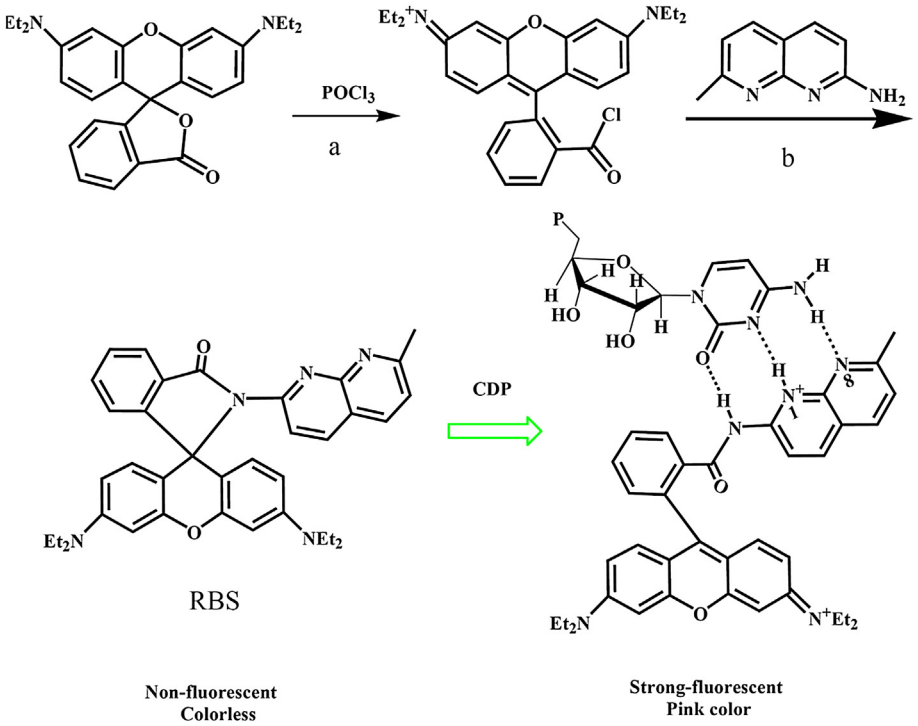

Scheme 1. The synthesis of **RBS** and the colorimetric and fluorescent sensing **CDP**. a. $ClCH_2CH_2Cl$; b CH_3CN, triethylamine.

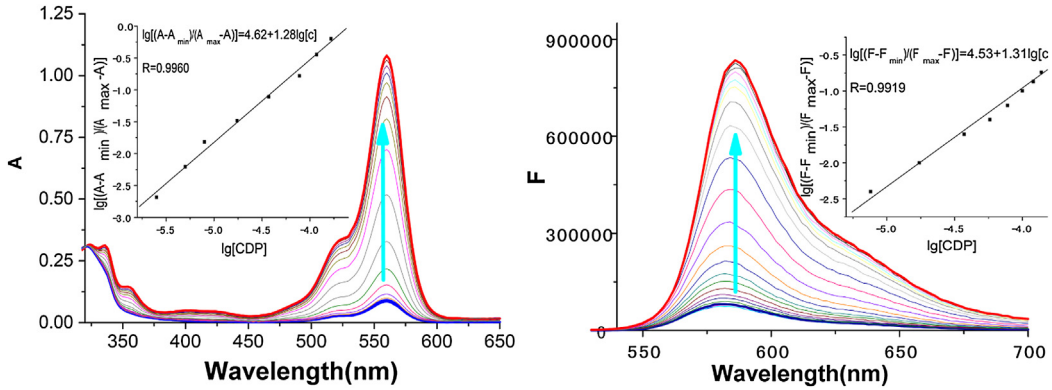

Fig. 3. UV spectra (left) and fluorescence spectra (right) of **RBS** (10 μM) upon the addition of 34 eq **CDP** in Tris–HCl buffer solution (pH 6.04 20 mM methanol/H_2O, 4/1, v/v). The inset shows the Benesi–Hildebrand fitting of the titration curve, intensity was recorded at λ_{em}: 586 nm (λ_{ex} = 540 nm), λ_{ab}: 560 nm.

dependency assay (Fig. 2). It is expected that complementary hydrogen bonding between nucleobase of related nucleotide polyphosphates and 2-aminonaphthyridine will be formed in such a pH range, which could induce spiroamide open lactone ring, consequently, the formation of 1:1 complexation species could be anticipated.

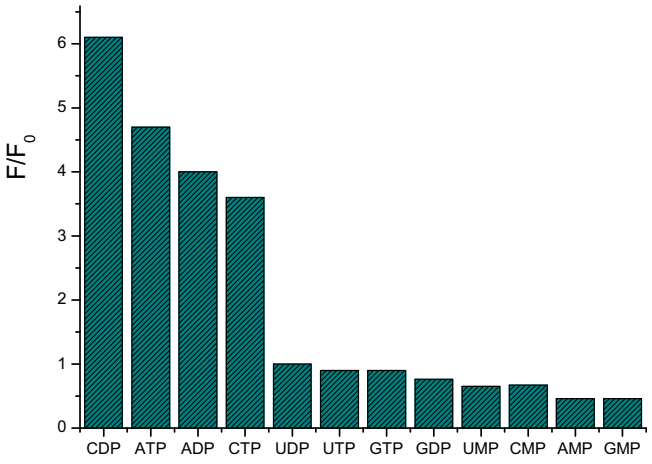

Fig. 4. Fluorescence response of **RBS** (10 μM) in methanol/H_2O (4/1, v/v) solution containing 20 mM pH = 6.04 Tris upon addition of ribonucleotide polyphosphates (0.20 mM) (excitation at 550 nm).

3.2. Absorption and fluorescence studies toward nucleotide polyphosphates

The free **RBS** in methanol/H_2O (4/1, v/v) containing 20 mM Tris buffer solution shows faint absorption at 560 nm and weak fluorescence (excitation at 560 nm) (right part of Fig. 3) which attributed to the partly opened spirolactam configuration, even though the solution remains almost colorless. As an aliquot of **CDP** stock solution was added, an absorption of the peak around 560 nm was significantly enhanced up to log ε = 5.04, following the significant color change of the solution from colorless to pink, suggesting the formation of the ring-opened tautomer of **RBS** upon **CDP** recombinating, which is also verified by the ^{1}H NMR splitting off at δ = 6.41 ppm. **RBS** thus could be served as convenience for detection nucleotides in aqueous media by naked eye. Concomitantly, a characteristic rhodamine B emission band centered at 580 nm appeared from a pale background upon the addition of **CDP** in the above-mentioned solution (right part of Fig. 3). The nonlinear fitting of the titration curve suggested a stable 1:1 stoichiometry complexation species with the association constant (log K_{ass}) calculated as 4.53. And such the big association constant could be not only attributed to the strong multi-hydrogen bonding interaction between cytosine and AMND but also attributed to other non-covalent interaction, such as electrostatic interaction, anion–π interaction [22,27].

It should be here noted that responding sensitivity of **RBS** to nucleic acid cytosine (**CDP** or **CTP**) over the nucleic acid guanine (Fig. 4), which does not accord with the reported results that

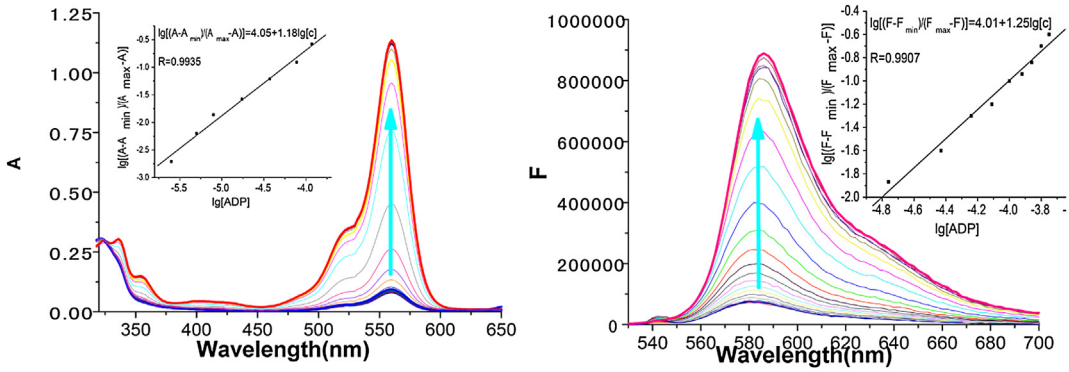

Fig. 5. UV spectra (left) and fluorescence spectra (right) of **RBS** (10 μM) upon the addition of 34 eq ADP in Tris–HCl buffer solution (pH 6.04 20 mM methanol/H_2O, 4/1, v/v). The inset shows the Benesi–Hildebrand fitting of the titration curve, intensity was recorded at λ_{em}: 586 nm (λ_{ex} = 540 nm), λ_{ab}: 560 nm.

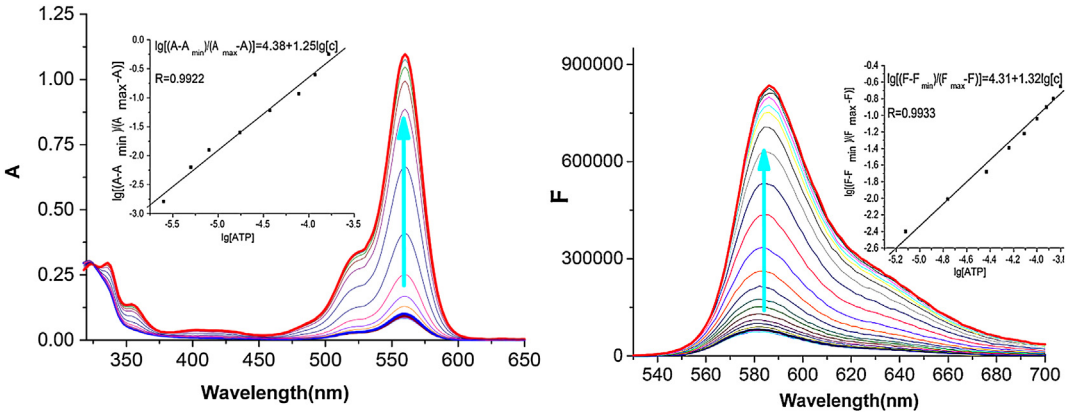

Fig. 6. UV spectra (left) and fluorescence spectra (right) of **RBS** (10 μM) upon the addition of 34 eq ATP in Tris–HCl buffer solution (pH 6.04 20 mM methanol/H_2O, 4/1, v/v). The inset shows the Benesi–Hildebrand fitting of the titration curve, intensity was recorded at λ_{em}: 586 nm (λ_{ex} = 540 nm), λ_{ab}: 560 nm.

amidation naphthyridine should prefer to bond to guanine due to the triple hydrogen bonding motif [28]. Such abnormal bonding affinity could be ascribed to the protonation of aminonaphthyridine under this pH conditions [3,4,29] which will prefer to form triple hydrogen bonding mode with the cytosine, as well as the steric effect [30].

The formation of hydrogen bond between the protonated aminonaphthyridine and related base was also exhibited in the well colorimetric and fluorescent response of **RBS** toward **ADP** (Fig. 5) and **ATP** (Fig. 6). It is reasonable to estimate that hydrogen bonding between protonated aminonaphthyridine and adenosine is feasible through two hydrogen bonds. Additionally, the weaker response of the probe to **XMP** might be due to that the spiroamide opening lactone ring accompanied by the parturition of imine positive ions, which is favorable to approach the polyphosphates anion by the electrostatic interaction. The variation of phosphoriboside linker length and steric configuration differentiate the electrostatic interaction ability.

3.3. MS and ^{1}H NMR studies for the complexation of *RBS* with nucleotide polyphosphates

ESI-MS spectra of CH_3CN solution **RBS** in the presence of 1 equal cytidine-5′-diphosphate disodium hydrate (**CDP**) exhibited a peak appears at *m*/*z* 1007.01, assignable to single-charged complex [**RBS** + CDP–Na]$^-$, and the peak intensity distribution exactly corresponds with the simulation on the basis of natural isotopic abundances, confirming the formation of the 1:1 complexation species (Fig. 7) between **RBS** and **CDP**.

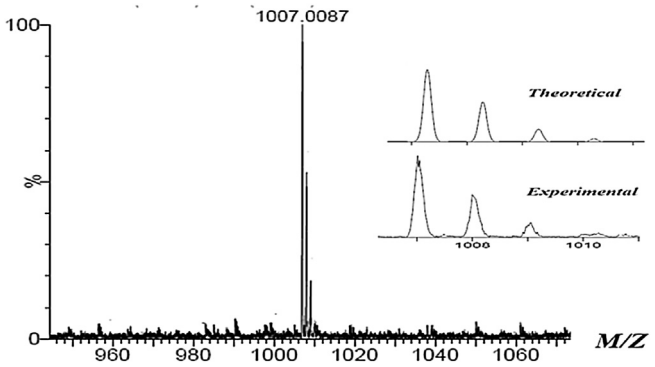

Fig. 7. ESI(-)-MS spectra of **RBS** after the addition of **CDP**. Insets: theoretical and experimental isotopic patterns at *m*/*z* 1007.2870, 1008.2870, 1009.2949 and 1010.2949.

The supramolecular hydrogen bond behavior of the titration solution was fully investigated by ^{1}H NMR spectrum (Fig. 8). The analysis of the ^{1}H NMR spectrum of **RBS** in DMSO/D_2O (4:1 v/v, and DCl) exhibits that naphthyridine portion of the spectrum is featured by four doublet at δ = 8.45 ppm (H3), 8.12 ppm (H2), 7.98 ppm (H4), 7.05 ppm (H1). Upon the addition of an appropriate amount of **CDP** into **RBS** in DMSO/D_2O (4/1, v/v) similar chemical shift was investigated referring to TMS as internal standard. H3 shifts to upfield with $\Delta\delta$ = 0.12 ppm, while H2 shifts to downfield with $\Delta\delta$ = 0.06 ppm. H15 on the cytidine base exhibits downshift ($\Delta\delta$ = 0.06 ppm). These results indicate the hydrogen bond interaction between **AMND** and base cytidine [31]. Importantly, multiplets of the xanthenes at δ = 6.41 split into two group peaks with different down field chemical shifts (see Fig. 8 marked as filled asterisk), such could suggest the opening up the spirolactam.

3.4. Preliminary cells imaging application

Furthermore, **RBS** exhibited the practical applicability as nucleotide polyphosphates probe in the fluorescent imaging in

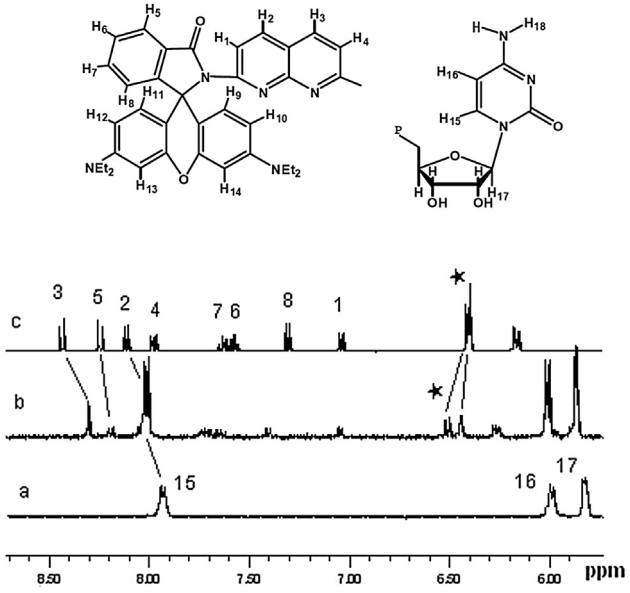

Fig. 8. Partial ^{1}H NMR spectra for (a) **CDP**, (b) **RBS** + **CDP** (2 eq), (c) **RBS** in d_6-DMSO/D_2O (4/1,v/v, and DCl), respectively.

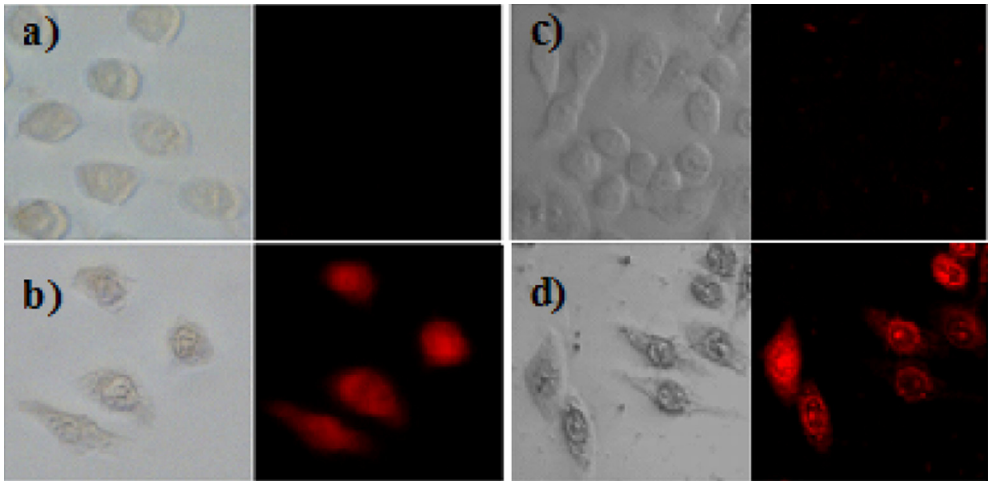

Fig. 9. Fluorescence images of HeLa cells (excited with green beam) incubated with **RBS** (10 μM) (a),(c) and their images after further incubated with **CDP** (b) and **ATP** (d), respectively.

living cells. HeLa cells were incubated with 10 μM **RBS** buffer solution (pH = 6.04) for 30 min at room temperature to allow the probe to permeate into the cells. When exciting at 510 nm, cells showed no obvious intracellular fluorescence (Fig. 9(a) and (c)). The cells stained with solution containing the probes were washed three times with physiological brine, and then incubated with nucleotide polyphosphates solution (pH = 6.04) for another 30 min, a significant fluorescence emission in live cells was observed (Fig. 9(b) and (d)). Bright-field measurement confirmed that the cells were viable throughout the imaging experiments after treatment with the probes and nucleotide polyphosphates solution.

4. Conclusions

In conclusion, we have developed a novel colorimetric and fluorescent sensor for nucleotide polyphosphates in water system. The probe exhibits good bonding affinity to cytidine and adenosine nucleoside tri/di-polyphosphates over the guanine polyphosphates, and it could be used in cell imaging of related nucleoside polyphosphates with strong emission response.

Acknowledgments

The authors thank the National Basic Research Program of China (2013CB733702) and NSFC (21102014).

Appendix A. Supplementary data

Supplementary data related to this article can be found at http://dx.doi.org/10.1016/j.dyepig.2013.10.002.

References

[1] Zimmermann H. Purinergic signaling in neural development. Semin Cell Dev Biol 2011;22:194–204.
[2] Yegutkin GG. Nucleotide- and nucleoside-converting ectoenzymes: important modulators of purinergic signalling cascade. Biochim Biophys Acta Mol Cell Res 2008;1783:673–94.
[3] Kobori A, Horie S, Suda H, Saito I, Nakatani K. The SPR sensor detecting cytosine–cytosine mismatches. J Am Chem Soc 2004;126:557–62.
[4] Yoshimoto K, Nishizawa S, Minagawa M, Teramae N. Use of abasic site-containing DNA strands for nucleobase recognition in water. J Am Chem Soc 2003;125:8982–3.
[5] Peng T, Dohno C, Nakatani K. Bidirectional control of gold nanoparticle assembly by turning on and off DNA hybridization with thermally degradable molecular glue. Chem Bio Chem 2007;8:483–5.
[6] Nakatani K, Horie S, Saito I. Affinity labeling of a single guanine bulge. J Am Chem Soc 2003;125:8972–3.
[7] Squire LR. Encyclopedia of neuroscience. New York: Academic Press; 2009.
[8] Zhou Y, Xu Zh, Yoon J. Fluorescent and colorimetric chemosensors for detection of nucleotides, FAD and NADH: highlighted research during 2004–2010. Chem Soc Rev 2011;40:2222–35.
[9] Chen X, Pradhan T, Wang F, Kim JS, Yoon J. Fluorescent chemosensors based on spiroring-opening of xanthenes and related derivatives. Chem Rev 2012;112:1910–56.
[10] Yang Y, Zhao Q, Feng W, Li F. Luminescent chemodosimeters for bioimaging. Chem Rev 2013;113:192–270.
[11] Kim HN, Lee MH, Kim HJ, Kim JS, Yoon J. A new trend in rhodamine-based chemosensors: application of spirolactam ring-opening to sensing ions. Chem Soc Rev 2008;37:1465–72.
[12] Beija M, Afonsoa CAM, Martinhoa JMG. Synthesis and applications of rhodamine derivatives as fluorescent probes. Chem Soc Rev 2009;38:2410–33.
[13] Zheng H, Zhan X, Bian Q, Zhang X. Advances in modifying fluorescein and rhodamine fluorophores as fluorescent chemosensors. Chem Commun 2013;49:429–47.
[14] Brown EV. 1,8-Naphthyridines. I. Derivatives of 2- and 4-methyl-1,8-naphthyridines. J Org Chem 1965;30:1607–10.
[15] Herranz F, Santa Maria MD, Claramunt RM. Molecular recognition: improved binding of biotin derivatives with synthetic receptors. J Org Chem 2006;71:2944–51.
[16] Folling J, Belov V, Kunetsky R, Medda R, Schonle A, Egner A, et al. Photochromic rhodamines provide nanoscopy with optical sectioning. Angew Chem Int Ed 2007;46:6266–70.
[17] Belov VN, Bossi ML, Folling J, Boyarskiy VP, Hell SW. Rhodamine spiroamides for multicolor single-molecule switching fluorescent nanoscopy. Chem Eur J 2009;15:10762–76.
[18] Jun ME, Ahn KH. Fluorogenic and chromogenic detection of palladium species through a catalytic conversion of a rhodamine B derivative. Org Lett 2010;12:2790–3.
[19] Zhou K, Liu H, Zhang S, Huang X, Wang Y, Huang G, et al. Multicolored pH-tunable and activatable fluorescen nanoplatform responsive to physiologic pH stimuli. J Am Chem Soc 2012;134:7803–11.
[20] Zhu H, Fan J, Xu Q, Li H, Wang J, Gao P, et al. Imaging of lysosomal pH changes with a fluorescent sensor containing a novel lysosome-locating group. Chem Commun 2012;48:11766–8.
[21] Lee MH, Han JH, Lee JH, Park N, Kumar R, Kang C, et al. Two-color probe to monitor a wide range of pH values in cells. Angew Chem Int Ed 2013;52:6206–9.
[22] Jorgensen WL, Pranata J. Importance of secondary interactions in triply hydrogen bonded complexes: guanine–cytosine vs uracil-2,6-diaminopyridine. J Am Chem Soc 1990;112:2008–10.
[23] Guerra CF, Bickelhaupt FM, Snijders JG, Baerends EJ. Hydrogen bonding in DNA base pairs: reconciliation of theory and experiment. J Am Chem Soc 2000;122:4117–28.
[24] Sponer J, Leszczynski J, Hobza P. Structures and energies of hydrogen-bonded DNA base pairs. A nonempirical study with inclusion of electron correlation. J Phys Chem 1996;100:1965–74.
[25] Sponer J, Leszczynski J, Hobza P. Nature of nucleic acid-base stacking: nonempirical ab initio and empirical potential characterization of 10 stacked

base dimers. Comparison of stacked and H-bonded base pairs. J Phys Chem 1996;100:5590–6.
[26] Corbin PS, Zimmerman SC. Self-association without regard to prototropy. A heterocycle that forms extremely stable quadruply hydrogen-bonded dimers. J Am Chem Soc 1998;120:9710–1.
[27] QuiÊonero D, Garau C, Rotger C, Frontera A, Ballester P, Costa A, et al. Anion–π interactions: do they exist? Angew Chem Int Ed 2002;41:3389–91.
[28] Nakatani K, Sando S, Saito I. Recognition of a single guanine bulge by 2-acylamino-1,8-naphthyridine. J Am Chem Soc 2000;122:2172–7.
[29] Sato Y, Nishizawa S, Yoshimoto K, Seino T, Ichihashi T, Morita K, et al. Influence of substituent modifications on the binding of 2-amino-1,8-naphthyridines to cytosine opposite an AP site in DNA duplexes: thermodynamic characterization. Nucleic Acids Res 2009;37:1411–22.
[30] Nishizawaa S, Yoshimotoa K, Seinoa T, Xu C, Minagawaa M, Satake H, et al. Fluorescence detection of cytosine/guanine transversion based on a hydrogen bond forming ligand. Talanta 2004;63:175–9.
[31] Bencini A, Biagini S, Giorgi C, Handel H, Baccon ML, Mariani P, et al. A Tris-macrocycle with proton sponge characteristics as efficient receptor for inorganic phosphate and nucleotide anions. Eur J Org Chem 2009;32:5610–21.